Functional analysis of the human rib cage over the vital capacity range in standing position using biplanar X-ray imaging

Claudio Vergari [1], Wafa Skalli [1], Louis Clavel [1,2], Michel Demuynck [1], Rémi Valentin [1,2], Baptiste Sandoz [1], Thomas Similowski [2,3], Valérie Attali [1,2,4]

1 Arts et Métiers Institute of Technology, Institut de Biomécanique Humaine Georges Charpak, Université Sorbonne Paris Nord, Paris, France.

2 Sorbonne Université, INSERM, UMRS1158 Neurophysiologie Respiratoire Expérimentale et Clinique, Paris, France.

3 AP-HP, Groupe Hospitalier Universitaire APHP-Sorbonne Université, site Pitié-Salpêtrière, Département R3S, Paris, France.

4 Groupe Hospitalier Universitaire APHP-Sorbonne Université, site Pitié-Salpêtrière, Service des Pathologies du Sommeil, Département R3S, Paris, France

Address:	Claudio VERGARI, PhD xx Institut de Biomécanique Humaine Georges Charpak Arts et Métiers 151 bd de l'Hôpital, 75013 Paris France	Tel:	+33 (0) 1 44 24 63 63
Email:	c.vergari@gmail.com ; claudio.vergari@ensam.eu		

Abstract word count: 219

Word count: 4132

Number of figures: 5

Number of tables: 1

Abstract

Pathologies of the respiratory system can by accompanied by alterations of the biomechanical function of the rib cage, as well as of its morphology and movement. The assessment of such pathologies could benefit from rib cage kinematic analysis during breathing, but this analysis is challenging because of the difficulties in observing and quantifying bone movements in vivo. This work explored the feasibility of using biplanar x-rays to study rib cage modifications at different lung volumes and evaluated the potential of the method to characterize rib cage kinematic patterns in patients.

Forty-seven asymptomatic adults and eleven obstructive sleep apnea syndrome (OSAS) patients underwent biplanar x-rays at three lung volumes: normal breathing, maximal and minimal volume. Rib cage and spinopelvic positional parameters were computed from 3D reconstruction of the skeleton.

Results showed that inspiration mostly mobilized the ribs and costo-vertebral junction, while expiration was driven by the spine. OSAS patients had a different sagittal profile at rest than asymptomatic subjects, but these differences decreased at maximal and minimal volume. This suggests that patients employed different biomechanical strategies to attain a trunk configuration similar to asymptomatic subjects at minimal and maximal lung volume.

This study confirmed that the proposed method could have an impact for the clinical assessment and understanding of pathologies involving breathing function, and which directly affect rib cage morphology.

Keywords: biomechanics, radiography, 3D reconstruction, breathing.

Introduction

Breathing, the biomechanical action of inhaling and exhaling through the lungs, is one of the most common activities for humans. The biological and physiological aspects of respiration, i.e, gas exchange in the lungs [1], and pulmonary function are well known. Several studies have focused on biomechanical modelling of breathing [2–4], but the experimental study of breathing presents several challenges. For instance, the changes in rib cage volume and shape during the breathing cycle are often analysed experimentally using only external measurements, in vitro approaches or animal models [5–11].

Actioned by respiratory muscles, rib cage modifications during breathing allow lung inflation and forceful exhalation. These modifications include rotation of the ribs around the medio-lateral and aneteroposterior axes of the rib cage, referred to respectively as the "pump-handle" orientation [12] and the "bucket-handle" orientation. Furthermore, rotation of the ribs around the vertical axis results in a widening or narrowing of the rib cage.

Rib movements have previously been quantified experimentally with functional analysis approaches, typically by acquiring radiographic images of the chest at different lung volumes. Sharp et al. [13] used lateral radiographs to measure rib sagittal orientation in 2D. More recently, Beyer al. used computerized tomography (CT) scans at three different volumes for functional analysis of the ribs in 3D [14,15]. However, while informative, these techniques are not compatible with routine clinical practice due to the high radiation dose and the necessity for patients to be supine for CT scanning.

Low-dose biplanar radiology (Figure 1) can be a valid alternative: it provides simultaneous posteroanterior and lateral radiographs while in a standing position and in a calibrated space, which allows 3D digital reconstruction of the bones [16]. It is performed in a standing position which offers the advantages of a chest examination closest to physiology and a simultaneous evaluation of spinopelvic parameters. Moreover, it may be repeated at several lung volumes to approach the changes of the rib cage and spine anatomy during breathing.

Several pathologies can alter rib cage movement during breathing. For instance, trunk deformities such as scoliosis affect the geometry of the rib cage, and therefore its function, which can result in respiratory impairment [17,18]. Conversely some chronic respiratory diseases are associated with alterations of the rib cage geometry which can results in spine deformations. In other pathologies, the relationship between geometry and function is less clear. For instance, obstructive sleep apnea syndrome (OSAS) is a chronic respiratory

pathology characterized by poor stability of upper airways, which leads to their recurrent obstruction during sleep [19]. OSAS patient do not present any lung or chest wall injury, nor specific bone structure deformity. Nevertheless, alterations of spine curvatures have been reported in these patients, particularly cervical hyperextension, which makes it easier to breathe while awake [20]. This hyperextension is often compensated with thoracic hyperkyphosis which has a potential impact on the rib cage and on its kinematics.

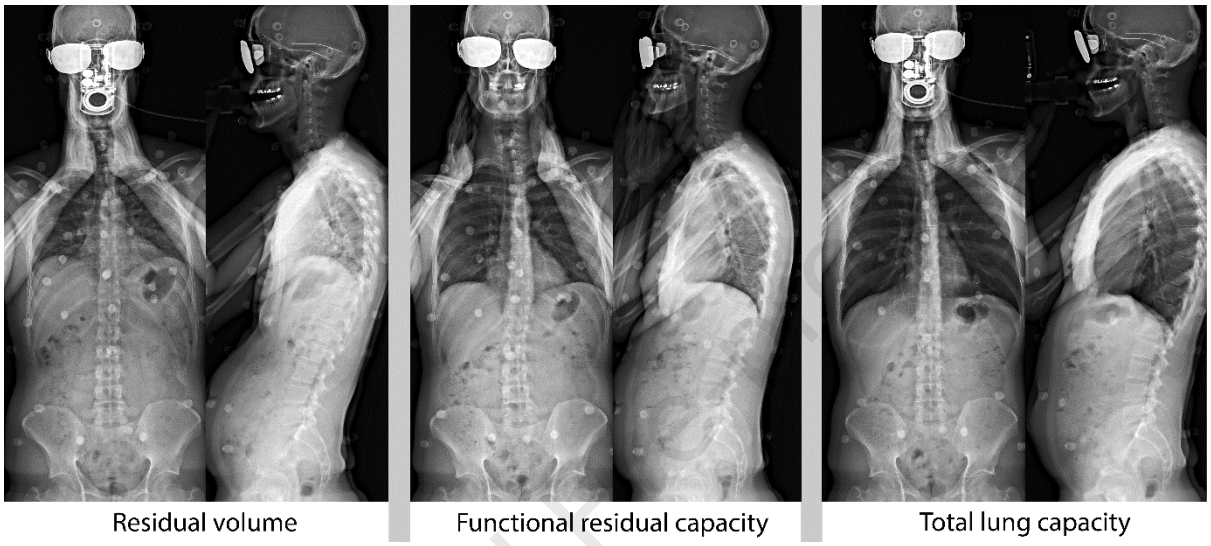

Figure 1. Biplanar x-rays of one 40-year-old healthy male subject at residual volume (minimal volume), functional residual capacity (relaxation volume) and total lung capacity (maximal volume).

In this context, the aim of this work was to determine the feasibility of functional analysis of the rib cage and the spine at several lung volumes using biplanar radiographs, and to evaluate the method in healthy subjects and in a small number of OSAS patients.

Methods

Subjects and imaging

Healthy subjects and OSAS patients were included at a single site in this prospective study. The study was approved by the appropriate ethics committee (Comité de Protection des Personnes (CPP) Ouest V for patients and the CPP Ile de France VI for healthy subjects). All participants signed an informed consent form.

Healthy subjects with normal pulmonary function test were included. Non-inclusion criteria were antecedents of musculoskeletal, respiratory, or neurological pathologies, previous surgery of the spine, rib cage or hip, supernumerary vertebrae or pregnancy. Patients in the OSAS group

were included with a diagnosis of moderate to severe OSAS, based on a polysomnography and symptoms. A subgroup of healthy subjects was also constituted by matching their age, weight, and height to OSAS patients for matched comparisons.

All participants underwent low-dose biplanar radiographs, which were performed using an x-ray slot-scanning imaging device (EOS, EOS Imaging, Paris, France) to obtain simultaneous antero-posterior and lateral images [16]. Radiographs were acquired with the participant in a free-standing position [21]: the participant was standing naturally, gaze forward, elbows fully flexed with fingers resting on the cheek bones (Figure 1). This position facilitates the subject's natural posture and improves visibility of spine and rib cage in both views. Subjects wore radiation protection eyewear.

A reference acquisition (approximately 10 seconds) was performed while the participants were breathing normally, which was considered to be representative of functional residual capacity (FRC). Subsequent acquisitions were performed after full exhalation (residual volume, RV) and after full inhalation (total lung capacity, TLC), during short apneas. RV and TLC maneuvers were driven by a pneumologist: a spirometer was used during the acquisition to ascertain that TLC and RV correspondent to the actual maximal and minimal lung volume for the subject..

3D reconstruction

The spine, pelvis and rib cage of all participants were reconstructed in the three lung volumes (FRC, RV, TLC) using previously validated methods [22,23]. Briefly, anatomical landmarks were manually annotated in both anteroposterior and lateral views. Then, a statistical algorithm provided an initial solution for the 3D reconstruction of the anatomical regions, which was retro-projected over the radiographs [22,23]. Finally, the 3D models were fine-adjusted manually, by deforming the model using control points, so that their contours corresponded to the radiographs. Thoracic and lumbar vertebrae were reconstructed (T1 to L5), and the ribs between 1 and 10; however, the first rib was excluded from the analysis because of the difficulty in correctly modeling its trajectory. Spinopelvic parameters (T1-T12 kyphosis, L1-L5 lordosis, pelvic tilt) were computed automatically from the 3D reconstruction [23]. The 3D reconstruction was obtained using custom in-house software, while the following calculations were done using Matlab R2021a (The Mathworks, Natick, MA, USA)

Computation of rib cage parameters

First, an anatomical coordinate system was defined: the vertical axis corresponded to the absolute vertical direction, the lateral axis was the vector joining the right to left pelvic acetabula, and the postero-anterior axis was the cross product of the previous two vectors.

The rib cage width was calculated at all vertebral levels as the maximum lateral distance between each pair of ribs. Rib cage volume was defined as the volume enclosed by a closed surface mesh through all the ribs [24].

A local reference system was then associated to each rib (Figure 2B): the vertical direction was the normal to a plane approximating the rib trajectory; the postero-anterior direction was the vector connecting the rib insertion to its bony tip, and the lateral direction resulted from the cross-product of the first two. Similarly, a local frame was associated to each pair of ribs (Figure 2C).

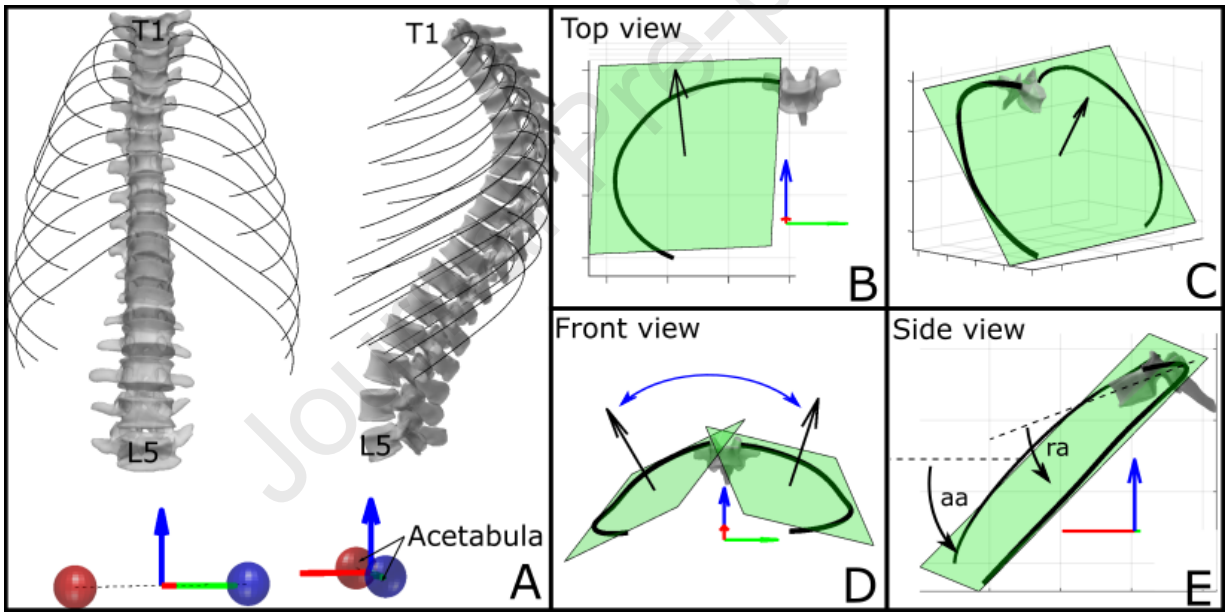

Figure 2. (A) 3D reconstruction of the spine, rib cage and pelvic acetabula. Planes were associated with each rib (B) and each pair of ribs (C) to calculate their orientations. The angle between two ribs in the coronal plane (D) was defined as “umbrella angle”, corresponding to the sum of the two “bucket-handle” angles. In the sagittal plane (E) the orientation of the ribs relative to the horizontal was computed (“aa”, corresponding to the average “pump-handle” angle), as well as the relative angle between the ribs and the vertebra (“ra”).

The orientation of these coordinate systems relative to the subject’s anatomical reference was evaluated by computing successive rotations around the lateral direction, then the local sagittal direction and local axial direction (LSA-L, [25]).

Rib orientation was used to compute the "umbrella angle", i.e., the angle between two ribs in the coronal plane (Figure 2D). The reference system associated to each pair of ribs was used to compute their sagittal orientation (Figure 2E). Angles relative to the vertebrae were computed by associating a robust coordinate system to each vertebra [23].

Animations

Animations of the vital capacity range were generated from functional data by linearly interpolating the movement of all bony structures between acquisitions. The following sequential phases were animated: from RV to FRC to TLC (inspiration from minimum to maximum lung volume), and back to FRC and RV (full expiration to minimum lung volume).

Reliability and statistics

Pilot data allowed to estimate that a cohort of 44 participants would have yielded a statistical power of 0.9 (calculated with GPower [26]) to detect a statistical difference between lung volumes. The comparison between healthy subjects and patients is a secondary objective, which is meant to produce pilot data for further studies.

To evaluate correlations between spinal and rib cage parameters, average orientation values were calculated for the ribs in the high (ribs 2-4), medium (ribs 5-7) and lower (ribs 8-10) portions of the rib cage. Correlations were quantified using Spearman's rank, while the comparisons of parameters between different lung volumes were calculated using Friedman's test for paired non-normally distributed data, followed by Tukey-Kramer post-hoc analysis. Data were compared for OSAS patients and height-, weight- and age-matched healthy subjects using Mann-Whitney tests. Non-parametric tests were preferred because not all variables were normally distributed, according to Lilliefors tests. Significance was set at $p < 0.05$. Results are reported as median [1st and 3rd quartiles].

Reliability was assessed using data from a cohort that were previously published in a study reporting different rib cage parameters [22]. This cohort included 20 adolescents (15 ± 2 years old) with mild to severe idiopathic scoliosis (Cobb angle 43° ± 11°) who underwent biplanar radiography in free-standing position. 3D reconstructions were performed twice by four experienced operators, for a total of 160 reconstructions. Reliability of the rib cage parameters was assessed according to the 5725 ISO standards, and inter-operator uncertainty was reported in terms of standard of deviation.

Results

In the following sections, "inspiration" is the change from functional residual capacity (FRC) to total lung capacity (TLC) and "expiration" is the change from FRC to residual volume (RV).

Study participants

Forty-seven healthy adults and eleven OSAS patients were included. Healthy subjects were 21 female and 26 males, aged between 20 and 83 years (33 [25, 48] years old, median [quartiles]). Median height was 1.72 [1.65, 1.76] m, and median weight 71 [61, 78] kg. Body mass index was 24 [21, 26] kg/m². OSAS patients were 7 males and 4 females; age 53 [52; 62] years; height 1.7 m [1.6, 1.8], weight 79 kg [73, 91]; apnea-hypopnea index/h 32 [28; 45]. Matched healthy subjects had median age 49 [47; 59] years, height 1.7 m [1.7, 1.7], weight 73 kg [67, 78]. OSAS patients and matched subject did not show differences in age, height or weight ($p > 0.05$).

Uncertainty of rib cage parameters

Uncertainty of sagittal absolute and relative angles was lower than 3.5° at all rib levels, while uncertainty of the umbrella angle was lower than 5.6°. Uncertainty of rib cage width was lower than 3 mm at all levels. Uncertainty tended to be higher at upper (ribs 1-2) and lower (ribs 9-10) levels for all parameters, but the differences in uncertainty were lower than 2° (2 mm for rib cage width).

Spinopelvic parameters

Table 1 presents spinopelvic parameters for the three lung volumes (RV, FRC, and TLC). In healthy subjects, T1-T12 kyphosis increased significantly on expiration and decreased on inspiration. Lumbar lordosis did not significantly change between lung volumes. Pelvic tilt decreased significantly on expiration and increased only slightly (albeit significantly) on inspiration. In OSAS patients, only T1-T12 kyphosis significantly changed between lung volumes.

Table 1. Spinopelvic parameters in three lung volumes. Values are reported as median [1st and 3rd quantiles]. RV = Residual volume, FRC = Functional residual capacity, TLC = Total lung capacity, Δ = Differences between lung volumes. * p<0.05, †p<0.01, ‡ p<0.001.

Parameter	RV	FRC	TLC	Difference
		Healthy subjects		
T1-T12 kyphosis °	63.1 [54; 67]	51.1 [44; 59]	46.6 [37; 56]	‡TLC < FRC ‡TLC < RV
L1-L5 lordosis °	-44.3 [-53; -35]	-44.4 [-56; -38]	-44.3 [-52; -39]	
Pelvic tilt °	15.8 [11; 22]	11.2 [8; 16]	12.9 [8; 17]	*TLC > FRC †TLC < RV ‡FRC < RV
		OSAS patients		
T1-T12 kyphosis °	67.6 [55; 75]	62.2 [49; 70]	46.5 [45; 66]	‡TLC < RV
L1-L5 lordosis °	-41.7 [-48; -35]	-44.6 [-47; -38]	-40.2 [-47; -34]	
Pelvic tilt °	14.5 [12; 20]	15.8 [12; 22]	16.7 [12; 20]	
		Matched healthy subjects		
T1-T12 kyphosis °	63.1 [62; 64]	54.1 [41; 59]	46.6 [41; 56]	†TLC < FRC *TLC < RV
L1-L5 lordosis °	-41.7 [-50; -39]	-43.3 [-47; -41]	-42.3 [-50; -39]	
Pelvic tilt °	19 [14; 22]	12.5 [11; 15]	14.9 [11; 17]	*TLC > RV ‡FRC > RV

Rib cage parameters in healthy subjects

Rib cage width and its variation between lung volumes are shown in Figure 3. With FRC values as reference, width was lower in RV and higher in TLC. However, differences were only significant between FRC and TLC at lower vertebral levels (between rib 7 and 10, $p < 0.05$). Increases up to 40 mm and decreases of 20 mm were observed.

Volumes at RV and FRC were similar (7.2 [5.9; 8.4] L vs 7.8 [6.1; 8.6] L) while volume at TLC was significantly higher (10.9 [7.7; 11.0] L, $p = 0.035$).

Figure 4a shows the sagittal orientation angles ("pump-handle" angles) of the ribs in the three lung volumes. Significant differences were present at all rib levels and between all three lung volumes ($p < 0.05$). However, the decrease in inspiration was much higher than the increase in expiration. Furthermore, the latter change was almost constant at all rib levels (5° median), while the change orientation in full inspiration was higher at the higher rib levels (-16°) than at the lower ones (-8°).

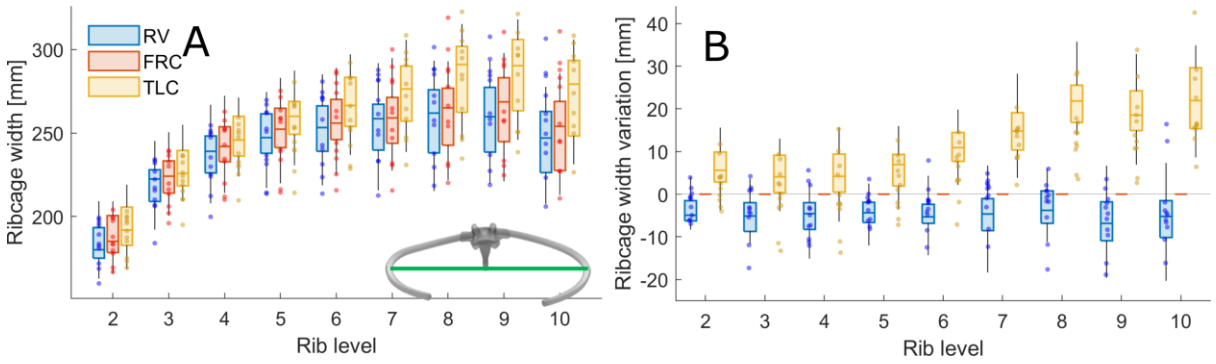

Figure 3. Rib cage width at lung residual volume (RV), functional residual capacity (FRC) and total lung capacity (TLC) is shown in panel A, while the variation from the reference state (FRC) is shown in panel B. Box plots represent median and 1st and 3rd quartiles for healthy subjects, with whiskers representing 95% interval. Data points represent OSAS patient.

Supplemental animation #1 shows the animation of the breathing cycle for a patient with large variation of sagittal angle, to highlight the rib cage modifications due to this rib movement.

Rib sagittal orientation angle relative to the vertebra is shown in Figure 4c. This angle increased monotonically from rib 2 to 10, indicating that ribs were almost aligned to the vertebra T1 (small angles), but had a large downward angle in T10, where the vertebra can be horizontally or upwards oriented. Although variations up to ±15° were measured in expiration, median values were close to zero. On the contrary, sagittal relative orientation significantly decreased at all levels during inspiration.

Figure 5 shows the umbrella angle and its variations. In all three conditions, values were lower in the mid thorax (T5-T8) than in the upper (T1-T4) and lower thorax (T9-T10). Angles at RV and FRC were similar ($p > z0.05$), while angles at TLC were significantly lower at all levels. This indicates that ribs were more coplanar during full inspiration, but their relative orientation in the coronal plane did not significantly change at full expiration.

Supplemental animation #2 shows the animation of a subject with large variations of the umbrella angle, which can be seen in the frontal view.

Correlations between rib cage and spinopelvic parameters in healthy subjects

T1-T12 kyphosis was correlated to rib sagittal relative orientation in the high and lower portions of the rib cage for all lung volumes (RV, FRC, TLC, $p < 0.05$), but not to the middle ribs. Kyphosis was not correlated to rib absolute sagittal orientation.

Kyphosis at rest was correlated with the variation of kyphosis between rest and RV (Spearman's rho = -0.7, $p < 0.0001$) and with the variation between rest and TLC (Spearman's rho = 0.-7, $p < 0.0001$).

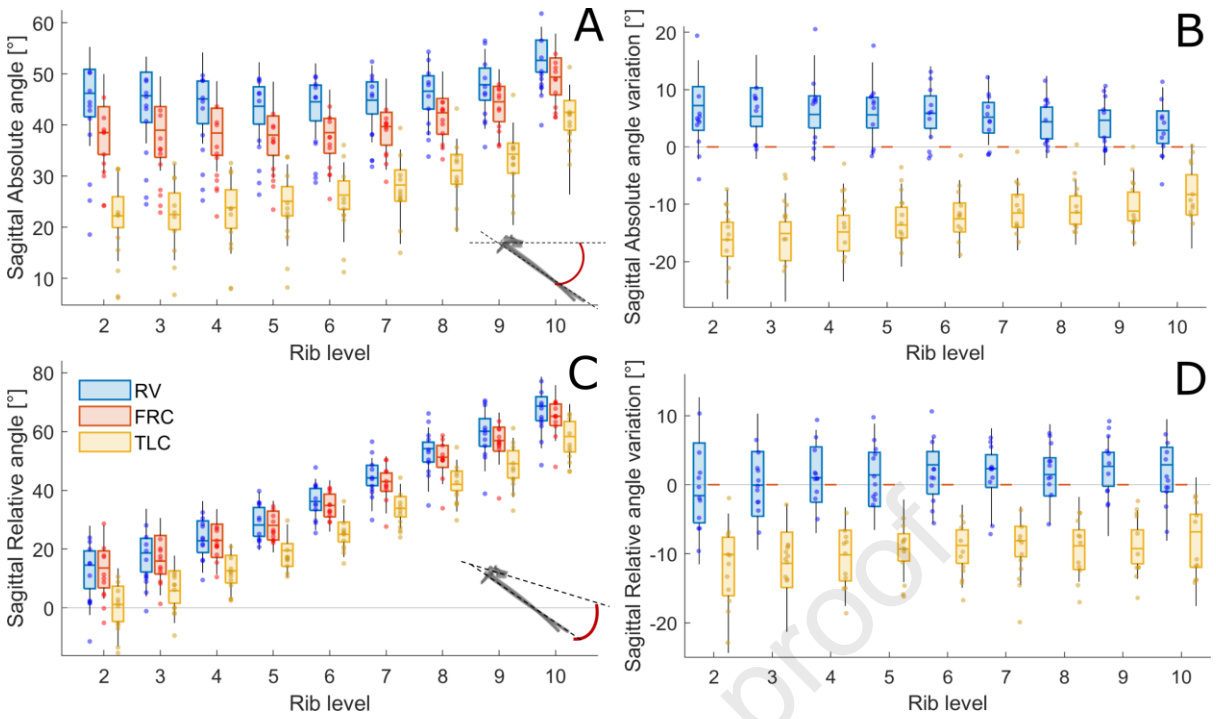

Figure 4. Orientation of the ribs in the sagittal plane relative to the horizontal (absolute angles, panel A) and relative to the vertebra (relative angles, panel C) at lung residual volume (RV), functional residual capacity (FRC) and total lung capacity (TLC). Variation from the reference state (FRC) are shown in the panels B and D. Box plots represent median and 1st and 3rd quartiles for healthy subjects, with whiskers representing 95% interval. Data points represent OSAS patient.

L1-L5 lordosis was correlated to sagittal relative orientation of the lower ribs ($p < 0.05$) for all lung volumes. In RV and FRC, lordosis was also correlated to absolute rib orientation.

Rib cage parameters did not significantly change with age. T1-T12 kyphosis significantly increased with age ($p < 0.05$), while lordosis and pelvic parameters did not change.

Comparison between OSAS patients and healthy subjects

OSAS patients showed normal rib cage width at rest (Figure 3) but tended to a reduced increase in width during inspiration: the width of 17% of rib pairs in OSAS patients increased less than the 95th percentile of healthy subjects.

OSAS patients also had an altered sagittal profile: Figure 4 shows that 24% of OSAS patients' ribs had a lower sagittal absolute angle than healthy subjects' 95th percentile in RV, and more than 10% ribs in FRC and TLC, i.e., the ribs of OSAS patients were more horizontal. Counterintuitively, sagittal relative angles between ribs and vertebrae were similar between OSAS patients and healthy subjects, as well as T1-T12 kyphosis ($p > 0.05$, Table 1).

Supplemental animation #3 shows a comparison between an asymptomatic subject with median kyphosis at rest (54°) and an OSAS patient with high kyphosis (77°).

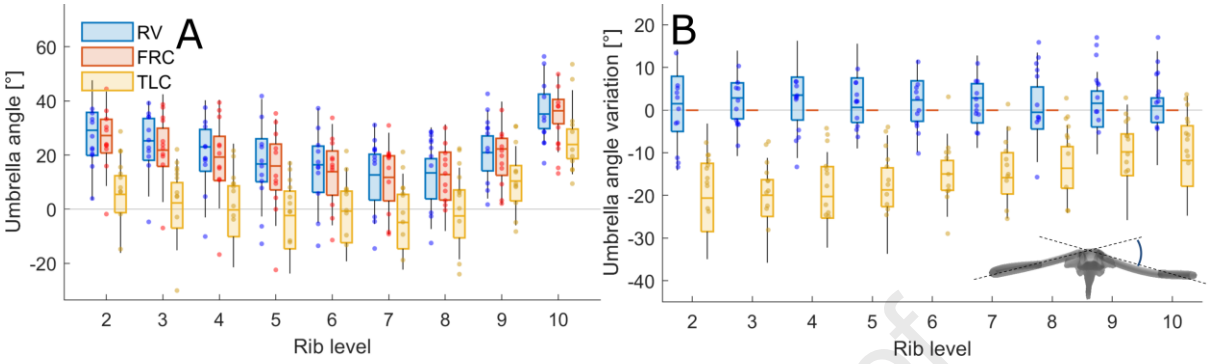

Figure 5. "Umbrella angle", i.e. the coronal angle between ribs at lung residual volume (RV), functional residual capacity (FRC) and total lung capacity (TLC) is shown in panel A, while variation from the reference state (FRC) is shown in the panel B. Box plots represent median and 1st and 3rd quartiles for healthy subjects, with whiskers representing 95% interval. Data points are reported for each OSAS patient.

When compared to matched healthy subjects, OSAS patients had slightly higher kyphosis at FRC (62.2° [49; 70] versus 54.1° [41; 59], Table 1), but the difference was not significant (p = 0.1). This lack of significance might be due to the small cohort size, since more than half OSAS patients (N=6) had a higher kyphosis than the 95th percentile of matched healthy subjects (59°). The difference in kyphosis between groups was reduced to less than 5° at RV and TLC. The pattern of kyphosis change was similar between OSAS patients and healthy subjects (Figure 4), although OSAS patients had a larger change between FRC and TLC than healthy subjects, and smaller change between FRC and RV (Table 1). In the coronal plane, umbrella angle was similar between groups (Figure 5).

Supplemental animation #3 shows the comparison of an OSAS patient with hyperkyphosis and a healthy subject. During maximal expiration, the healthy subject increases his kyphosis with a backward shift of the spine while the OSAS patient pushes the spine forward inside the rib cage. However, this strategy was also observed in healthy subjects with high kyphosis as attested by the negative correlation between kyphosis at the FRC and the change of kyphosis at full expiration.

Discussion

We used 3D functional analysis to describe the behavior of the rib cage and spinopelvic parameters during upright breathing, with extreme lung volume variations, in healthy subjects and OSAS patients. Unlike their ribcage, an analysis of spine and pelvis of these participants was previously published [27]. The originality of this work lies in the use of pseudo-dynamic biplanar x-rays acquisitions to estimate the modifications of the rib cage and spine during breathing.

Reproducibility was consistent with a similar study using lateral radiographs for ribs 4 to 7 (3°) [13]. In this previous study, sagittal angles were measured relative to a vertical axis, unlike the present work where a horizontal axis was used. Nevertheless, the results can be compared by applying a transformation of 90°-x, where x represents the results of the previous study. In this way, both studies showed an absolute sagittal angle increasing slightly from rib 4 to 7, and ribs sloping downwards progressively from RV to FRC to TLC. There was a systematic difference of about 10° between the two studies, which is explained by the different measuring methods.

Our results are also consistent with Wilson et al. [12], who measured sagittal angles between 40 and 50° (from rib 2 to 9) at FRC and 25° to 40 at TLC. The sum of left and right "bucket angle" measured by Wilson et al. should correspond to the "umbrella angle" measured in the present work. However, orientations in the present work were calculated using rotation matrices, which yield more consistent results than measuring projected 2D angles, especially when measuring large angles [28]. In the present study, pairs of ribs were coplanar in TLC (umbrella angle ≈ 0°), while they were at an angle between 15 and 35° in RV and FRC, according to different rib levels (Figure 5).

The analysis of sagittal absolute angles suggested large downward reorientation of the ribs during inspiration, with variations of -12°, and smaller upwards reorientation in expiration (~5°). Relative angles showed very small variation during expiration, and larger downward reorientation during inspiration. This is also shown in Supplemental animation #1, which shows that the changes between FRC and TLC are mainly due to a reorientation of the ribs, while the expiration from FRC to RV is characterized by a backward movement of the whole trunk and changes in spinal sagittal alignment.

This suggests that maximum inspiration is mainly characterized by rib cage and costovertebral movements, while forced expiration is obtained with a penetration of the spine within the rib cage and a translation of the whole trunk. This is corroborated by the small changes measured

in rib cage volume between RV and FRC, which suggests that lung volume was further reduced by the abdominal contents being pushed by abdominal muscles. Different muscular synergies are deployed during the two breathing phases: inspiration is mainly driven by the diaphragm, which is helped by external intercostal muscles for maximal inspiration. Full expiration is obtained with the abdominal muscles and internal intercostal muscles [1]. Diaphragmatic component of the respiration was not accounted for in the present work because the diaphragm position was not evaluated. In particular, volume estimation from 3D reconstruction of the rib cage leads to an overestimation of lung volume at RV, when the diaphragm is high in the thoracic cavity.

Interestingly, thoracic kyphosis significantly changed between lung volumes, while lumbar lordosis was almost constant, so the change in thoracic alignment was not compensated by the lumbar spine. This might due to the stiffening effect that the diaphragm, the intra-abdominal pressure and trunk muscle activity have on the lumbar spine during extreme variations of lung volumes [29]. On the other hand, changes of thoracic curvature are facilitated and accompanied by rib motion.

OSAS patients showed slightly higher kyphosis at the FRC than matched healthy subjects, albeit not significantly. Moreover, OSAS patients showed a specific pattern of rib cage characteristics. A third of the patients had a significantly small sagittal orientation of the ribs, i.e., their ribs were more horizontal than healthy subjects. Given that relative angles between ribs and vertebrae were similar in the two groups, it can be hypothesized that patients and healthy subjects differ in the rib cage orientation in space, rather than cage morphology. Conversely both groups had similar kyphosis at full inspiration and expiration, indicating a difference in terms of spinal and rib cage kinematics over the range of volume variation during vital capacity. Kyphosis was reduced more in OSAS patients than healthy subjects from FRC to TLC (16° versus 7°) and increased less from FRC to RV (5° versus 9°). This suggests that OSAS patients and healthy subjects deploy different strategies to reach extreme volumes from the FRC.

Additional investigations are needed to determine if OSAS and hyperkyphosis are independent predictors of the rib cage morphology and the related expiration behaviour. However, our results support the existence of an adapted rib cage kinematics in OSAS, even in patients with normal respiratory function, and suggest a link between the upper airway instability in OSAS and the adaptation of the rib cage kinematic. The relationship between this altered rib cage kinematic and the altered perception of respiratory sensations that was previously shown in

OSAS patients [30] remains putative and needs to be further explored. However, the present study showed that the proposed method could be integrated in routine clinical practice, because of the low dose of radiation delivered to the patient and an examination protocol that can easily be reproduced. The reconstruction method to obtain the geometry of spine and rib cage was previously described in the literature, and the novelty of this work is the definition and analysis of geometrical parameters.

This work has some limitations. First, the methodology of the acquisition should be considered when interpreting the results, particularly the interpolated animations provided as supplemental material. Second, the conditions analysed (maximal variations of lung volume, breath holding) do not necessary reflect the biomechanics of natural breathing at rest and might amplify or distort the normal rib cage kinematics. Third, measurement uncertainty should be considered when interpreting the results. Fourth, diaphragm shape and position were not characterized in this work, and rib cage volume was estimated from the surface enclosing only the ribs 1 to 10 [24]. This approximation might be realistic during inspiration when the diaphragm is relatively flat but is less accurate during expiration when the diaphragm is dome shaped. However, such approximation of rib cage volume is strongly correlated to lung volume at FRC, as measured through pulmonary functional testing [31]. Future research could assess the relationship between "radiological" rib cage volumes and functional lung volumes. Finally, a limited sample of only eleven OSAS patients were included, but the aim of this work was to provide a proof of concept, to be applied in larger cohorts of patients in future evaluations. Besides, age, sex and height effects were not explored, although preliminary analyses show that age and height have a higher impact on rib cage kinematics than sex; for this reason, patients and healthy subjects were matched by these parameters and not by sex.

This study underlines the relation between spinal alignment and therefore balance and the rib cage, with thoracic spine and rib cage morphologies being highly related. Particularly, hyperkyphosis was associated with an adaptation of the rib cage kinematic over extreme lung volume variations, of which the impact on pulmonary function remains to be studied. This should be taken into account in the elderly, due to the high frequency of hyperkyphosis in this population. In OSAS patients, our results suggest a link between their upper airway instability and an adapted thoracic cage kinematics. These results also encourage the integration of systematic postural and respiratory assessments in OSAS patients or suspected OSAS, even in those with normal lung function. More generally, it would be effective to investigate postural adaptations and rib cage kinematics in some other chronic respiratory diseases with lung

hyperinflation, e.g. chronic obstructive pulmonary disease, and to explore their changes before and after a targeted treatment.

Conclusion

This work confirmed the feasibility of assessing rib cage functional analysis with low-dose biplanar x-rays, through radiological acquisitions in standing load-bearing position at different stages of breathing. The method allowed the quantification of 3D rib cage morphology at different lung volumes, giving a novel insight into the biomechanics of breathing and the strategies deployed by the subject to attain lung volumes.

Results of this work confirm that both the spine and the rib cage are largely involved in maximal inspiration and expiration, but also that their action is asymmetrical: inspiration mostly mobilized the ribs and costo-vertebral junction, while expiration was driven more by the spine. The present work describes a novel approach to the functional examination of the rib cage, with a potential impact for a large panel of patients.

Acknowledgements

The authors are grateful to the BiomecAM chair program on subject-specific musculoskeletal modelling (with the support of ParisTech and Yves Cotrel Foundations, Société Générale, Covea and Proteor). We are also grateful to Andrew Lang for English editing.

Role of the funding source

Nothing to disclose.

Conflict of interest statement

Dr. Skalli has a patent related to biplanar X-rays and associated 3D reconstruction methods, with no personal financial benefit (royalties rewarded for research and education) licensed to EOS Imaging. The other authors have nothing to disclose.

Author contributions

W.S., B.S., T.S and V.A. designed the research. L.C., M.D. and R.V. acquired the data. WS, MD, LC, BS and C.V. designed and developed new software. C.V. verified and processed the data, and drafted the work. All authors participated in the data analysis and interpretation, and all revised the manuscript. All authors approved the submitted version.

Supplemental animations legends

Supplemental animation #1. Animation of the breathing cycle for a patient with large variation of sagittal angle, to highlight the rib cage modifications due to this rib movement.

Supplemental animation #2. Animation of a subject with large variations of the umbrella angle, which can be seen in the frontal view.

Supplemental animation #3. Comparison between an asymptomatic subject with median kyphosis at rest (54°) and an OSAS patient with high kyphosis (77°).

References

[1] J.B. West, Respiratory Physiology, Wolters Kluwer | Lippincott Williams & Wilkins, 2012.

[2] S.A. Holcombe, A.M. Agnew, B. Derstine, S.C. Wang, Comparing FE human body model rib geometry to population data, Biomech. Model. Mechanobiol. 19 (2020) 2227–2239. https://doi.org/10.1007/s10237-020-01335-2.

[3] S.A. Holcombe, S.C. Wang, J.B. Grotberg, Modeling female and male rib geometry with logarithmic spirals, J. Biomech. 49 (2016) 2995–3003. https://doi.org/https://doi.org/10.1016/j.jbiomech.2016.07.021.

[4] S.B. Ricci, P. Cluzel, A. Constantinescu, T. Similowski, Mechanical model of the inspiratory pump, J. Biomech. 35 (2002) 139–145. https://doi.org/https://doi.org/10.1016/S0021-9290(01)00164-6.

[5] A. De Troyer, M. Estenne, Coordination between rib cage muscles and diaphragm during quiet breathing in humans, J. Appl. Physiol. 57 (1984) 899–906. https://doi.org/10.1152/jappl.1984.57.3.899.

[6] J.M. Lopes, E. Tabachnik, N.L. Muller, H. Levison, A.C. Bryan, Total airway resistance and respiratory muscle activity during sleep, J. Appl. Physiol. 54 (1983) 773–777. https://doi.org/10.1152/jappl.1983.54.3.773.

[7] A.S. Jordan, D.P. White, Y.-L. Lo, A. Wellman, D.J. Eckert, S. Yim-Yeh, M. Eikermann, S.A. Smith, K.E. Stevenson, A. Malhotra, Airway Dilator Muscle Activity and Lung Volume During Stable Breathing in Obstructive Sleep Apnea, Sleep. 32 (2009) 361–368. https://doi.org/10.1093/sleep/32.3.361.

[8] A. Ratnovsky, D. Elad, P. Halpern, Mechanics of respiratory muscles, Respir. Physiol. Neurobiol. 163 (2008) 82–89. https://doi.org/https://doi.org/10.1016/j.resp.2008.04.019.

[9] A. De Troyer, T.A. Wilson, Action of the diaphragm on the rib cage, J. Appl. Physiol. 121 (2016) 391–400. https://doi.org/10.1152/japplphysiol.00268.2016.

[10] I. Chu, C. Fernandez, K.A. Rodowicz, M.A. Lopez, R. Lu, R.D. Hubmayr, A.M. Boriek, Diaphragm muscle shortening modulates kinematics of lower rib cage in dogs, Am. J. Physiol. Regul. Integr. Comp. Physiol. 299 (2010) R1456–R1462. https://doi.org/10.1152/ajpregu.00016.2010.

[11] C. Liebsch, N. Graf, H.-J. Wilke, In vitro analysis of kinematics and elastostatics of the human rib cage during thoracic spinal movement for the validation of numerical models, J. Biomech. 94 (2019) 147–157. https://doi.org/https://doi.org/10.1016/j.jbiomech.2019.07.041.

[12] T.A. Wilson, A. Legrand, P.-A. Gevenois, A. De Troyer, Respiratory effects of the external and internal intercostal muscles in humans, J. Physiol. 530 (2001) 319–330. https://doi.org/https://doi.org/10.1111/j.1469-7793.2001.0319l.x.

[13] J.T. Sharp, G.A. Beard, M. Sunga, T.W. Kim, A. Modh, J. Lind, J. Walsh, The rib cage in normal and emphysematous subjects: a roentgenographic approach, J. Appl. Physiol. 61 (1986) 2050–2059. https://doi.org/10.1152/jappl.1986.61.6.2050.

[14] B. Beyer, S. Van Sint Jan, L. Chèze, V. Sholukha, V. Feipel, Relationship between

costovertebral joint kinematics and lung volume in supine humans, Respir. Physiol. Neurobiol. 232 (2016) 57–65. https://doi.org/https://doi.org/10.1016/j.resp.2016.07.003.

[15] B. Beyer, V. Feipel, V. Sholukha, L. Chèze, S. Van Sint Jan, In-vivo analysis of sternal angle, sternal and sternocostal kinematics in supine humans during breathing, J. Biomech. 64 (2017) 32–40. https://doi.org/https://doi.org/10.1016/j.jbiomech.2017.08.026.

[16] J. Dubousset, G. Charpak, W. Skalli, J. Deguise, G. Kalifa, Eos: a new imaging system with low dose radiation in standing position for spine and bone & joint disorders, J. Musculoskelet. Res. 13 (2010) 1–12. https://doi.org/10.1142/S0218957710002430.

[17] S.L. Weinstein, D.C. Zavala, I. V Ponseti, Idiopathic scoliosis: long-term follow-up and prognosis in untreated patients., JBJS. 63 (1981). https://journals.lww.com/jbjsjournal/Fulltext/1981/63050/Idiopathic_scoliosis__long_term_follow_up_and.3.aspx.

[18] B. Schlager, F. Krump, J. Boettinger, R. Jonas, C. Liebsch, M. Ruf, M. Beer, H.-J. Wilke, Morphological patterns of the rib cage and lung in the healthy and adolescent idiopathic scoliosis, J. Anat. n/a (2021). https://doi.org/https://doi.org/10.1111/joa.13528.

[19] A.L. Lee, R.S. Goldstein, C. Chan, M. Rhim, K. Zabjek, D. Brooks, Postural deviations in individuals with chronic obstructive pulmonary disease (COPD), Can. J. Respir. Crit. Care, Sleep Med. 2 (2018) 61–68. https://doi.org/10.1080/24745332.2017.1409091.

[20] L. Clavel, S. Rémy-Neris, W. Skalli, P. Rouch, Y. Lespert, T. Similowski, B. Sandoz, V. Attali, Cervical Spine Hyperextension and Altered Posturo-Respiratory Coupling in Patients With Obstructive Sleep Apnea Syndrome, Front. Med. 7 (2020) 30. https://doi.org/10.3389/fmed.2020.00030.

[21] F.D. Faro, M.C. Marks, J. Pawelek, P.O. Newton, Evaluation of a functional position for lateral radiograph acquisition in adolescent idiopathic scoliosis, Spine (Phila Pa 1976). 29 (2004) 2284–2289. http://www.ncbi.nlm.nih.gov/pubmed/15480143.

[22] C. Vergari, B. Aubert, P. Lallemant-Dudek, T.-X. Haen, W. Skalli, A novel method of anatomical landmark selection for rib cage 3D reconstruction from biplanar radiography, Comput. Methods Biomech. Biomed. Eng. Imaging Vis. 8 (2020). https://doi.org/10.1080/21681163.2018.1537860.

[23] L. Humbert, J.A. De Guise, B. Aubert, B. Godbout, W. Skalli, 3D reconstruction of the spine from biplanar X-rays using parametric models based on transversal and longitudinal inferences, Med Eng Phys. 31 (2009) 681–687. https://doi.org/10.1016/j.medengphy.2009.01.003.

[24] B. Aubert, C. Vergari, B. Ilharreborde, A. Courvoisier, W. Skalli, 3D reconstruction of rib cage geometry from biplanar radiographs using a statistical parametric model approach, Comput. Methods Biomech. Biomed. Eng. Imaging Vis. 4 (2016) 281–295. https://doi.org/10.1080/21681163.2014.913990.

[25] B. Drerup, Principles of measurement of vertebral rotation from frontal projections of the pedicles, J. Biomech. 17 (1984) 923–935. https://doi.org/https://doi.org/10.1016/0021-9290(84)90005-8.

[26] E. Erdfelder, F. Faul, A. Buchner, GPOWER: A general power analysis program, Behav. Res. Methods, Instruments, Comput. 28 (1996) 1–11. https://doi.org/10.3758/BF03203630.

[27] V. Attali, L. Clavel, P. Rouch, I. Rivals, S. Rémy-Néris, W. Skalli, B. Sandoz, T. Similowski, Compensation of Respiratory-Related Postural Perturbation Is Achieved by Maintenance of Head-to-Pelvis Alignment in Healthy Humans , Front. Physiol. . 10 (2019) 441.

[28] W. Skalli, F. Lavaste, J.L. Descrimes, Quantification of three-dimensional vertebral rotations in scoliosis: what are the true values?, Spine (Phila Pa 1976). 20 (1995) 546–553. https://doi.org/10.1097/00007632-199503010-00008.

[29] D. Shirley, P.W. Hodges, A.E.M. Eriksson, S.C. Gandevia, Spinal stiffness changes throughout the respiratory cycle, J. Appl. Physiol. 95 (2003) 1467–1475. https://doi.org/10.1152/japplphysiol.00939.2002.

[30] V. Attali, J.-M. Collet, O. Jacq, S. Souchet, I. Arnulf, I. Rivals, J.-B. Kerbrat, P. Goudot, C. Morelot-Panzini, T. Similowski, Mandibular advancement reveals long-term suppression of breathing discomfort in patients with obstructive sleep apnea syndrome, Respir. Physiol. Neurobiol. 263 (2019) 47–54. https://doi.org/https://doi.org/10.1016/j.resp.2019.03.005.

[31] H. Bouloussa, R. Pietton, C. Vergari, T.X. Haen, W. Skalli, R. Vialle, Biplanar stereoradiography predicts pulmonary function tests in adolescent idiopathic scoliosis: a cross-sectional study, Eur. Spine J. 28 (2019) 1962–1969. https://doi.org/10.1007/s00586-019-05940-3.

Highlights

- Assessing the movement of the rib cage during breathing is still a challenge.
- Biplanar x-ray was used to measure rib cage morphology at three lung volumes.
- Different respiratory strategies were deployed by patients and healthy subjects.
- The proposed method offers a novel approach to functional examination of rib cage.

Conflict of interest statement

Dr. Skalli has a patent related to biplanar X-rays and associated 3D reconstruction methods, with no personal financial benefit (royalties rewarded for research and education) licensed to EOS Imaging. The other authors have nothing to disclose.